"Most of the fundamental ideas of science are essentially simple, and may, as a rule, be expressed in a language comprehensible to anyone".

***Albert Einstein** (1879–1955), German-born U.S. physicist.*
The Evolution of Physics (co-written with Leopold Infeld).

CHAPTER 2

FUNDAMENTAL CONCEPTS

2.1 INTRODUCTION.

This chapter reports on the literature concerned with the subject of the present work. Accordingly, concepts including conductive polymers, in-situ composites, flow of polymer melts and electrical conductivity, among others, will be reviewed in the relevant sections. In the same way, a special section is dedicated to polyaniline and related topics.

2.2 ELECTRICALLY CONDUCTIVE POLYMERS.

The conventional method for imparting electrical conductivity to common polymers is by admixing them with conductive solid fillers such as carbon black or metal particles. However, the relatively high filler content needed to yield high electrical conductivity may adversely affect the materials processability and other properties [3,4]. Therefore there is an increasing interest in using intrinsically conductive polymers (ICPs) to produce electro-conductive polymeric materials with an attractive combination of properties.

The common electronic feature in ICPs is the presence of conjugated double bonds (hence the term conjugated polymers) in which a π-conjugated system is formed by overlap of carbon p_z orbitals and alternating carbon-carbon bond lengths [5-7]. In some systems, however, notably polyaniline (PANI), nitrogen p_z orbitals and rings consisting of six carbon atoms are also part of the conjugation path [8,9].

Initially, ICPs were neither processable nor air stable mainly due to their chain structure and strong intermolecular interactions. However, later ICPs generations were processable into air stable powders, films and fibres following conventional methods such as solution and melt processing, respectively [10-19]. Moreover, the production of ICPs-based polymeric blends has also been achieved [11-13,16,20-24].

The electrical conductivities of ICPs systems now range from that typical of insulators (i.e., $< 1 \times 10^{-10}$ S/cm) and semiconductors such as silicon (ca. 1×10^{-5} S/cm), up to greater than 1×10^{4} S/cm (nearly that of a metal such as copper, i.e., 5×10^{5} S/cm) [25,26]. Applications of these polymers, especially PANI, have begun to emerge. These include blends with potential applications in energy storage [27], antistatic packaging

[28,29], electro-optical devices [16,30], welding of plastics [31], industrial textiles [28,32], etc.

Conjugated polymers as such are insulators. They possess an energy gap between filled and empty energy levels. However, their conductivities are transformed from insulating to conducting through doping [5-7,26,33]. In the doped state, the backbone of the conducting polymer consists of a delocalised π system. Both electron-donating and electron-accepting dopants have been used [25,34]. The doping is typically done using vapours or solutions of the dopant. Electrochemical methods have also been employed. In some circumstances, the polymer and the dopant are dissolved in the same solvent before forming the film, powder or fibre. The polymer backbone and dopant ions form a rich variety of new three-dimensional structures.

The charge-storage species formed upon doping are termed solitons, polarons and bipolarons [7,35]. For some conjugated polymers, the charges added to the backbone at low doping levels are stored in charged soliton and polaron states [6,7,36] or as charged bipolarons [37]. For other ICPs, high doping results in polarons interacting to form a polaron lattice (i.e., an electrically conducting partially filled energy band) [38,39]. Some models suggest equilibrium between polarons and bipolarons [40].

The first intrinsic electrically conducting organic polymer, doped polyacetylene (PA), was reported by Shirakawa et al. in 1977 [41,42]. The interest in PA, both theoretical and experimental, generated a prolific collection of data which led to the discovery that poly(*p*-phenylene) could also be doped to obtain high levels of conductivity [43]. It demonstrated that PA was not unique and led to the development of a number of new polyaromatic-based conducting systems such as poly(*p*-phenylene sulphide) [44], polypyrrole [45], polythiophene [46] and the aforementioned PANI [47].

2.3 POLYANILINE.

Polyaniline is presently one of the most promising intrinsically conductive polymers. Special interest has been focused on PANI due to a number of important reasons including its excellent chemical stability combined with relatively high levels of electrical conductivity that can be controlled. Additionally, the monomer (aniline) is

relatively inexpensive and its polymerisation, that is, the 1,4-oxidation of aniline in acidic media, is a straightforward high-yielding reaction [48-51].

2.3.1 STRUCTURE.

Studies on polyaniline suggest that the polymer can exist in a wide range of structures [5,49,52]. The polymer can be regarded as one composed of a random copolymer of reduced (amine) and oxidised (imine) units (fig. 2.1).

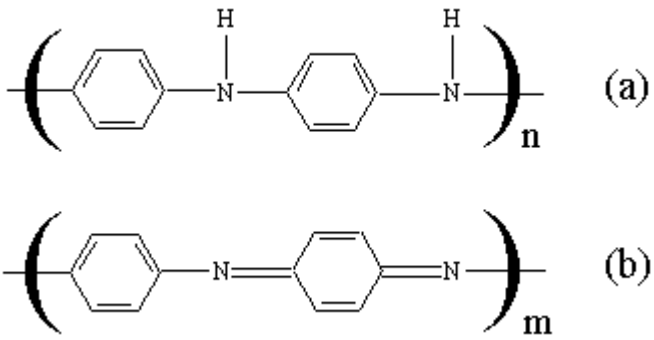

Figure 2.1. Amine (a) and imine (b) units of a polyaniline chain (n and m are integers).

For n $\neq$ 0 and m $\neq$ 0 (refer to fig. 2.1), the structures of polyaniline are known as the poly(*p*-phenyleneamineimines) in which the oxidation state of the polymer increases with increasing the content of the imine form. The fully reduced (i.e., m = 0) and oxidised (i.e., n = 0) forms are referred to as the leucoemeraldine and pernigraniline, respectively. On the other hand, the 50 % oxidised structure (i.e., n = m) is known as the emeraldine base (EB) of PANI. However, intermediate oxidation states have also been defined between these structures. Accordingly, protoemeraldine is known as the intermediate structure between leucoemeraldine and emeraldine, whereas nigraniline is defined as the intermediate structure between emeraldine and pernigraniline.

As has been indicated, the EB form of PANI is half-oxidised and thus consists of phenylendiamine and quinoid diimine units (fig. 2.2).

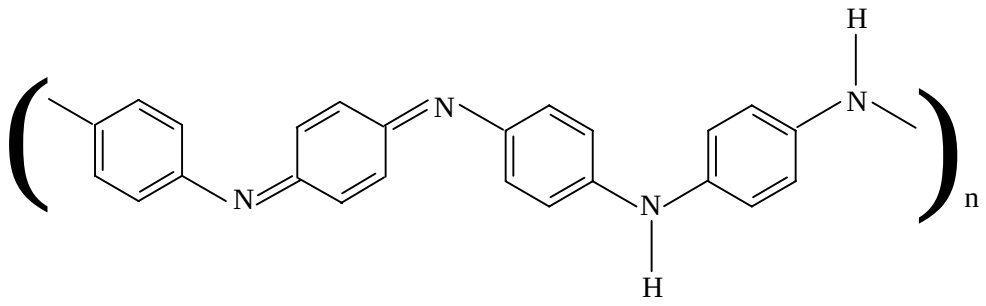

Figure 2.2. The emeraldine base of polyaniline.

The emeraldine base is insulating. However, its iminic nitrogen sites can be protonated by strong acids to form an acid-base complex [19,31,49,53-57]. This electrically conductive form is called the emeraldine salt (ES) of PANI. A fully protonated conductive complex is formed when about 0.5 mol of protonic acid, A^-H^+, per mol of phenyl-N repeat unit of PANI is used (fig. 2.3).

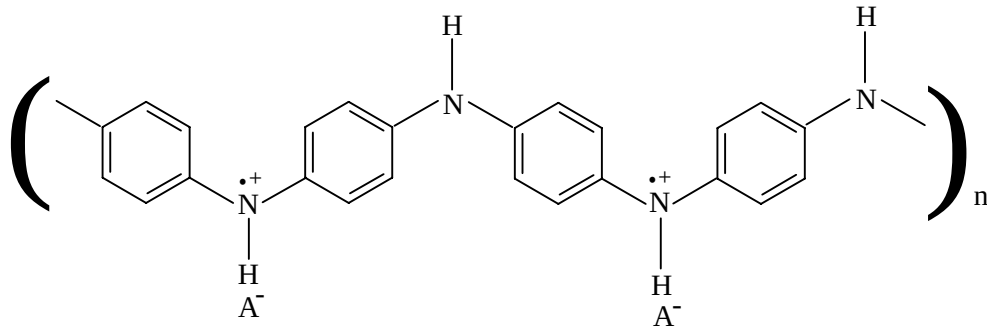

Figure 2.3. The emeraldine salt of polyaniline where A^- denotes a negatively charged molecular anion, that is, a counter-ion.

2.3.2 PROCESSABILITY.

The emeraldine base is soluble in *N*-methylpyrrolidone (NMP), selected amines, concentrated sulphuric acid and other strong acids [58-60]. However, the emeraldine salt is even more intractable and hence its processability is limited. This intractability is caused by its highly aromatic nature, the interchain hydrogen bonding and the charge delocalisation effects. Many methods have been developed to improve the processability. These include blending the ES with other polymers by using co-solvents

[57,58], preparing sterically stabilised colloidal dispersions [61,62] and chemically [11,56] or electrochemically [63] polymerising aniline within a polymer matrix.

Melt and solution processability can be improved if PANI is protonated with a functionalized protonic acid [64]. A functionalized protonic acid, denoted as $H^+(X^-R)$, consists of a protonic acid group (i.e., H^+X^-) and an organic group (i.e., R). The proton reacts with the imine nitrogens of PANI transforming the EB to the conducting salt form. The (X^-R) group serves as a counter-ion, where R, the functional group, enhances the solubility in common organic solvents and compatibility with conventional polymers. The solubility and compatibility in a given polymer are determined by the structure of the functional group. Well-known examples of such functionalized protonic acids are *p*-dodecylbenzenesulfonic acid (DBSA) [16,21,53,65,66], (±)-camphor-10-sulfonic acid (CSA) [16,65,67], bis(2-ethyl hexyl) hydrogen phosphate (DiOHP) [57,68] and diphenyl hydrogen phosphate (DPHP) [69].

2.3.3 SOLUTION PROCESSABLE COMPLEXES.

As has been pointed out, EB turns into processable electro-conductive solution complexes by using specific functionalised counter-ions. These complexes are soluble in common organic solvents such as toluene, chloroform, chlorobenzene, resorcinol, xylene, *m*-cresol, etc. [16,53,65-67,69]. Conductive products of pure PANI have been obtained by casting [16,53], dipping [70] or spinning [12,16,18] directly from solution with subsequent evaporation of the solvent. Hot pressing procedures after solvent evaporation have also been reported [69]. On the other hand, an approach based on the contact of the EB with an organic solvent (i.e., pyruvic acid) capable of protonating the polymer for the preparation of conductive polyaniline solutions has been reported [30]. In this process, dissolution and protonation of the emeraldine base were carried out simultaneously yielding true solutions of the conductive emeraldine salt.

2.3.4 SOLUTION PROCESSABLE BLENDS.

The solubility of the solution processable complexes (SPCs) of PANI in common organic solvents enables the fabrication of solution processable PANI blends using

different traditional non-conductive polymers and permits the blended material to be dissolved and processed from solution. Typical products are thin transparent films [16,57,67,68], coatings [30], inks [71], paints [66,71], fibres [12] and adhesives [71]. PANI SPCs can also be dissolved in some thermosetting matrices, such as phenol-formaldehyde and melamine resins, which are subsequently cured into the final product [71].

2.3.5 MELT PROCESSABLE COMPLEXES.

Melt processable PANI complexes have been obtained using a thermal doping process in which the EB and a specific functionalized acid (e.g., DBSA) are mixed at high temperature, which results in the formation of a PANI-DBSA conductive complex [21,72]. This method allows simultaneously doping EB and introducing alkyl substituents to its backbone without the need for using auxiliary solvents. The presence of unbound excess of DBSA, only physically mixed with PANI, leads to the dispersion of the PANI particles in the DBSA, which leads to the production of a paste mainly ionically conducting. Heating causes solidification of the paste, which becomes electrically conductive. If large amounts of excess of DBSA are used, an elasticised complex is then created. The addition of compatibility agents has also been reported [28].

2.3.6 MELT PROCESSABLE BLENDS.

Studies have been reported about preparation of electrically conductive PANI blends by melt processing techniques [14,21,22,28,31,66]. Among these, Shacklette et al. [22] report that Versicon (from Allied-Signal Inc.), a conductive form of PANI, was dispersible in polar thermoplastics such as polycaprolactone and poly(ethylene terephthalate glycol). On the other hand, Ikkala et al. [14] report on conductive polymer blends prepared by blending thermoplastic polymers with a PANI-DBSA complex following a thermal doping method in which conventional melt-processing techniques were used. Furthermore, Virtanen et al. [28] have given an account of the production of relatively homogeneous polymer blends from PANIPOL^{TM} (a conductive complex created by Neste Oy Chemicals) and non-polar plastics such as polyolefins,

polystyrenes, PVC, etc.. Additionally, Virtanen and co-workers indicate that PANIPOL^{TM} acts as a processing aid, that is, the melt viscosity and required processing temperature is generally lower for the blends than for the matrix polymers. This results in a decreased processing time, reduced scrap generation and lower energy costs.

2.3.7 ELECTRICAL PROPERTIES.

The final optimum properties of the electrically conductive PANI blends, specifically the electrical conductivity, depend on many parameters such as the content of PANI in the blend, the processing techniques, the processing parameters and the polymer matrix. Additionally, the methods used for doping PANI greatly affect the conductivity of the blend. Regardless of this, it has been found that the relationship between the room temperature conductivity and the content of PANI in the blends is characteristic of percolation threshold behaviour, with reasonable high levels of conductivity being observed even for composites containing relatively low conducting PANI loadings [11,21,56,57,66]. For example, Oh et al. [11] report on a percolation threshold in the range of 6-10 weight percent (wt%) of conductive PANI (fig. 2.4) in a PANI-polystyrene (PS) composite, which was chemically obtained by using DBSA as the doping agent in the presence of xylene. Moreover, they also indicate that a high level of conductivity of ca. 0.1 S/cm was achieved with only 12 wt% of the conductive component.

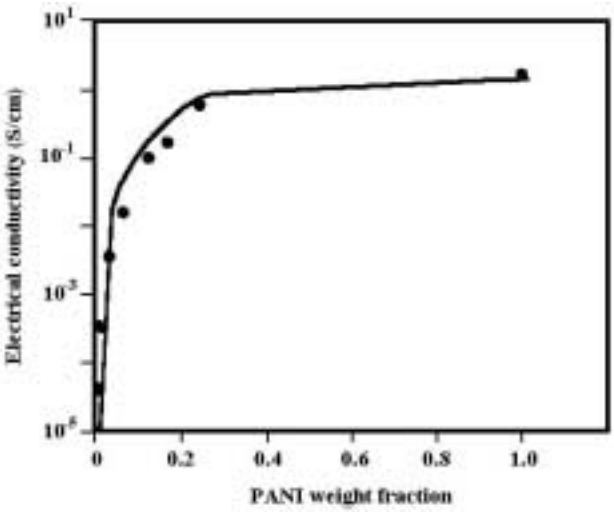

Figure 2.4. Electrical conductivity of PANI-PS composites as a function of PANI weight fraction (from Oh et al. [11]).

2.4 CONDUCTIVITY OF COMPOSITE MATERIALS.

This section concentrates on some of the theories and models available to describe the conductivity of composite materials. Although quantum-mechanical electron tunnelling effects between two closely conducting grains in an insulating matrix have been considered [73-76], it is the percolation theory together with effective media theories that have received the greatest attention. A brief insight into these theories is presented here, together with the description of other proposed models.

2.4.1 PERCOLATION.

The word percolate literally means *to pass through a filter* (e.g., to make a liquid or gas pass through a filter or porous substance, or filter through in this way). It also means *to pass through slowly* (e.g., to pass slowly through something or spread throughout a place) [77]. In the context of the present work, percolation refers to whether an electrical insulator containing an electrically conducting filler would allow the passage of an electrical current.

2.4.2 PERCOLATION THEORY.

Percolation theory provides an estimate of the probability of the existence of a conducting path through a system (or composite medium) as a function of the conducting filler volume fraction. It gives a phenomenological equation for the conductivity of the medium near to the metal-insulator (or conductor-perfect conductor) transition. Although the theory has largely been developed in the context of regular lattices, it is also used to describe the conductivity of continuum systems [78-80].

The two most common lattice percolation models are the site and bond percolation models, respectively. In the former model, random sites are missing from the lattice. On the other hand, the bond percolation model assumes that all the sites in the lattice are occupied, however not all the sites are connected. Although the two models are treated in a very similar way, the bond percolation model is very ambiguous, which led to the site percolation model to be used in preference even by many leading researchers, for example Stauffer and Aharony [79].

To understand the site percolation model, one must envisage a large array of squares as shown in figure 2.5a. This array should be imagined to be so large that any effects from its boundaries are negligible. Such an array is called a square lattice. Now, a certain fraction of squares are filled with a dot in the centre, whereas the other squares are left empty (fig. 2.5b). A cluster is now defined as a group of neighbour squares occupied by the dots. These clusters are encircled in figure 2.5c. From this picture it can be seen that squares are called nearest neighbours if they have a side in common but not if they only touch at one corner. Squares with one common side are defined as "nearest neighbour sites on the square lattice", whereas squares touching at one corner are called "next nearest neighbours". All sites within one cluster are thus connected to each other by one unbroken chain of nearest-neighbour links from one occupied square to a neighbour square also occupied by a dot. The occupation of the squares is random, that is, each square is occupied or empty independent of the occupation status of its neighbours. Each site has a probability P of being occupied by a dot, which means that if there are N squares, and N is a very large number, then PN of these squares are occupied, and the remaining $(1 - P)$N of these squares are empty. For values of P between zero and a critical value P_c, the situation is one of finite clusters as illustrated in fig. 2.5c.

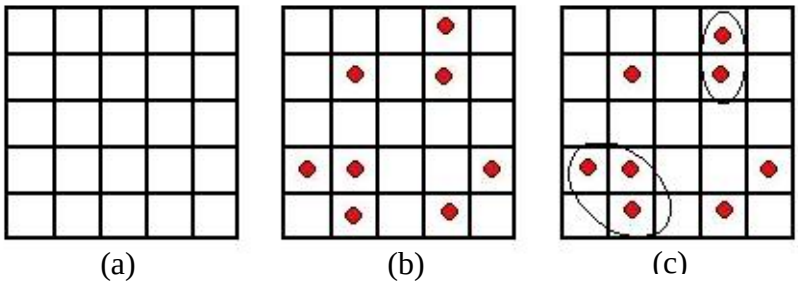

Figure 2.5. Site percolation model: (a) shows part of a square lattice; in (b) some squares are occupied with dots; in (c) the clusters, groups of neighbouring occupied squares, are encircled except when the cluster consists of a single square (from Stauffer et al. [79]).

In theory, the conductivity of the lattice can be measured by placing it between electrodes attached to its opposing faces. Because the finite clusters are not connected to each other (fig. 2.5c), the entire lattice is, at this stage, insulating. At exactly P_c for an infinite lattice (or very near these values for a very large lattice) an infinite conducting cluster is first formed. Because there is now a conducting or percolation path across the

entire lattice, the conductivity becomes finite. Above P_c the conductivity of the lattice (σ_m) is found to increase as $(P - P_c)^t$, where t is a dimensionless index, and P_c is the critical or percolation threshold. For lattices in three dimensions, t usually lies between 1.65 [81] and 2.0 [76], which is the accepted range of t demanded by universality.

The probability that a site will occur in the infinite conducting cluster, together with the conductivity of the cluster, are schematically plotted in fig. 2.6 as a function of the fraction of sites in the lattice.

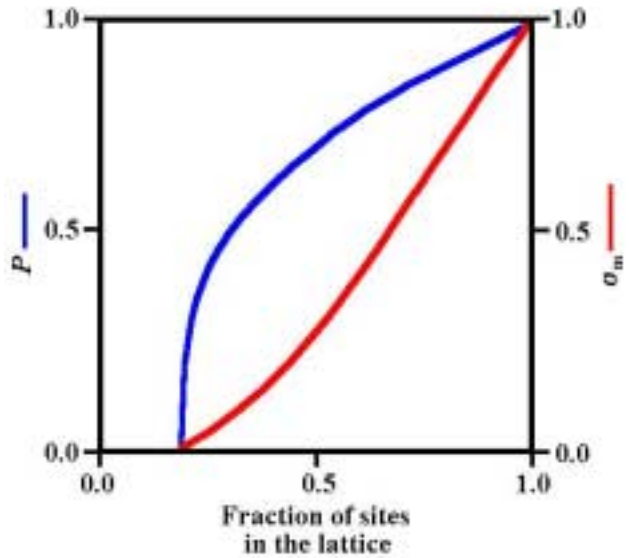

Figure 2.6. Typical behaviour of the conductivity (σ_m) of the infinite conducting cluster and the probability (P) of a site being in it as a function of the fraction of sites in the lattice (from Kirkpatrick [78], Stauffer et al. [79] and McLachlan et al. [80]).

As can be observed from fig. 2.6, at a fraction of sites equal to one, P is equal to 1. At this point, σ_m reaches a maximum value, which for convenience has been set equal to unity. However, the behaviour of σ_m and P near the percolation threshold is radically different. The reason for this difference is that, just above P_c, the vast majority of the sites in the infinite conducting cluster do not carry any current because they are situated on “dead ends” or “backwaters”. The actual array of sites that carries the current is known as the “backbone” [79,80]. This is illustrated in fig. 2.7, which shows a section of an infinite bond cluster on the square lattice at P_c. If each bond of this cluster represents a resistor, and if a voltage is put between the upper and lower ends of the cluster, then many bonds can be identified which will carry no current because they lead nowhere (i.e., the “dangling” bonds or “dead ends”). If all the dangling bonds are removed, what is left is the backbone. Every internal bond on the backbone has at least

two independent routes that lead from it to the edges of the cluster. Except for rare symmetric situations, all the backbone bonds will carry some current when a voltage is put between the upper and lower edges of the cluster. It has been demonstrated [79] that most of the mass of the infinite network at the percolation threshold belongs to dead ends, not to the backbone. Therefore, most of the mass contained in the conducting cluster makes no contribution to the conductivity, and hence the difference in the behaviour of σ_m and P.

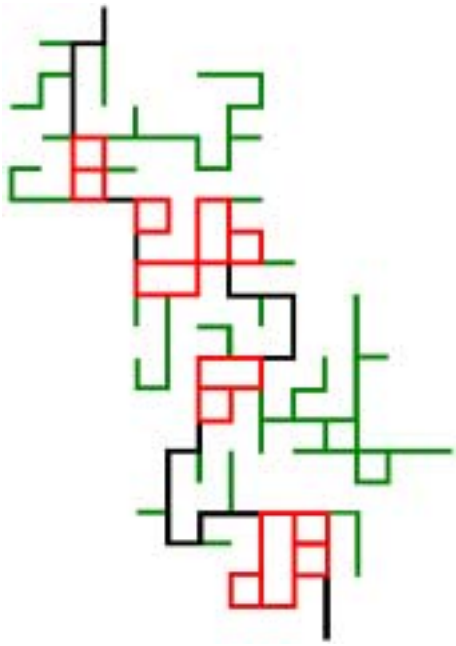

Figure 2.7. Section of an infinite cluster at P_c. Bond percolation model. Green lines represent "dangling" bonds, whereas black lines represent singly connected bonds. Red lines represent bonds on "blobs" (from Stauffer et al. [79]).

In continuous media or a continuum, which is the case most relevant to the subject of the present work, the percolation theory suggests that in the neighbourhood of the threshold the conductivity will be given by the following power-law equation [80,82]:

$$\sigma_m = \sigma_h(\phi - \phi_c)^t \text{.....} Eq.\ 2.1,$$

where:

σ_m = conductivity of the medium (or composite),

σ_h = conductivity of the conductive filler,

ϕ = volume fraction of the conductive filler,

ϕ_c = critical volume fraction of the conductive filler (percolation threshold),

t = critical exponent.

2.4.3 EFFECTIVE MEDIA THEORIES.

An effective media theory describes a binary (or higher) mixture as one consisting of ellipsoidal (or spherical) grains in which each grain is surrounded by a mixture that has the effective conductivity of the composite medium [80,83]. The simplest approach considers a two-phase dispersion consisting of spherical (or ellipsoidal) particles dispersed in a conducting medium, that is, *the Maxwell's dilute limit* (a review on the subject is given by Meredith et al. [84]). Other approaches include the *Bruggeman's symmetric and asymmetric effective media theories*, which have been reviewed by McLachlan et al. [80,85,86]. These approaches will be described next.

The dilute limit is illustrated in fig. 2.8, which depicts insulating ellipsoidal (or spherical) grains dispersed in a conducting matrix.

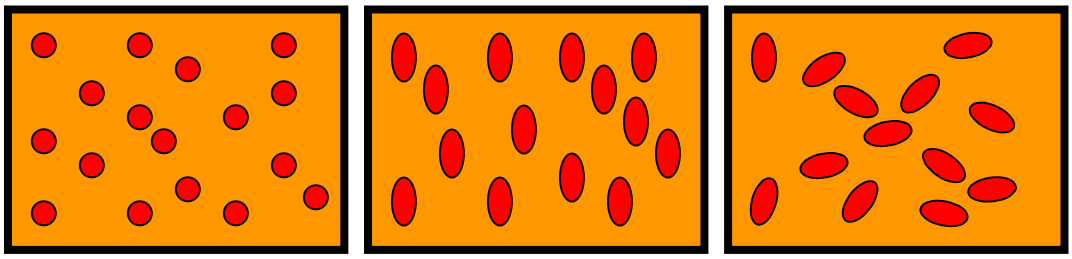

(a) **(b)** **(c)**

Figure 2.8. Maxwell's dilute limit for insulating spheres (a), insulating oriented ellipsoids (b) and randomly oriented ellipsoids (c) dispersed in a conducting matrix (from McLachlan et al. [80]).

Using Maxwell's equation, the conductivity of the composite medium represented in fig. 2.8 can be expressed as follows.

For spheres:

$$\sigma_m = \sigma_h \left(1 - \frac{3}{2} f\right) \text{.....} \textit{Eq. 2.2a.}$$

For oriented ellipsoids:

$$\sigma_m = \sigma_h \left(1 - \frac{f}{1 - L_f}\right) \text{.....} \textit{Eq. 2.2b.}$$

For randomly oriented ellipsoids:

$$\sigma_m = \sigma_h \left(1 - m_f f\right) \text{.....} \textit{Eq. 2.2c.}$$

In the equations presented above, as well as in other ones presented in this section, σ_m is the conductivity of the composite medium, σ_h the conductivity of the high-conductivity phase (i.e., the continuous phase in this particular case), f the volume fraction of the low-conductivity phase (i.e., the perfectly insulating dispersed phase), L_f the depolarisation coefficient for the oriented ellipsoids in the direction of the current flow [87], and m_f a coefficient that can be calculated in the limit where the conductivity of the low-conductivity phase, σ_l, is zero [84].

The complementary expressions used when perfectly (or infinitely) conducting particles (with resistivity $\rho = 0$) are immersed in a matrix with a finite conductivity are:

For spheres:

$$\rho_m = \rho_h(1-3\phi) \text{.....} \textit{Eq. 2.3a.}$$

For oriented ellipsoids:

$$\rho_m = \rho_h\left(1-\frac{\phi}{L_\phi}\right) \text{.....} \textit{Eq. 2.3b.}$$

For randomly oriented ellipsoids:

$$\rho_m = \rho_h(1-m_\phi\phi) \text{.....} \textit{Eq. 2.3c.}$$

In equations 2.3a to 2.3c ρ_m is the resistivity of the composite medium, ρ_h (i.e., $1/\sigma_l$) the resistivity of the high-resistive phase (in this case the continuous phase), ϕ the volume fraction of the conducting phase, L_ϕ the depolarisation coefficient of the oriented ellipsoids and m_ϕ a coefficient related to the randomly oriented ellipsoids. Note that $\rho_l = 1/\sigma_h$, the resistivity of the low-resistive phase (the dispersed phase in this case) is equal to zero. The symbols presented in *Eq. 2.3a* to *2.3c* will be used in other equations corresponding to this section. They will have the same meaning.

Equations 2.2a to 2.3c are valid up to volume fractions (f or ϕ) of about 0.1. Expressions for media where σ_l and ρ_l are not zero can be found in a number of references, for example Meredith et al. [84].

The Bruggeman's symmetric media theory [88] treats the two (or more) constituents with conductivities σ_l and σ_h and volume fractions f of σ_l and $1 - f = \phi$ of σ_h, on a completely symmetrical basis. The theory, which is based on the expressions for the polarization of a sphere, is for a random mixture of "spherical grains" of the two

constituents, in the correct volume ratio, which together completely fill the media. To visualize this *symmetric medium*, the entire composite medium must be assumed to be filled with oriented ellipsoids (or spheres), which implies an infinite size range of ellipsoids. The equation for the conductivity of a symmetric media, written in the more general form for oriented ellipsoids [89-91] is

$$\frac{f(\sigma_l - \sigma_m)}{\sigma_l + \left(\frac{1-L}{L}\right)\sigma_m} + \frac{(1-f)(\sigma_h - \sigma_m)}{\sigma_h + \left(\frac{1-L}{L}\right)\sigma_m} = 0 \text{ .....} \textit{Eq. 2.4.}$$

It must be noted that when the composite medium is composed of oriented ellipsoids it is anisotropic and that in *Eq. 2.4*, $L_f = L_\phi = L$. An isotropic medium is obtained only when $L_f = L_\phi = L = 1/3$ (spheres) [80].

The $(1 - L)/L$ term is more often written as $f_c/(1 - f_c)$ or $(1 - \phi_c)/\phi_c$, where $f_c = 1 - \phi_c$ and ϕ_c are the critical percolation thresholds of the low-conductive and high-conductive phases (already defined in section 2.4.2), respectively.

If $\sigma_l = 0$, then *Eq. 2.4* reduces to *Eq. 2.2b* and a metal-insulator transition occurs when $f = 1 - L_f$. For example, the critical volume fraction (f_c) for spheres is 2/3.

Equation 2.4 can be written in terms of the resistivities of the low and high-resistive phases, and the volume fraction, ϕ, of the low-resistive phase. In the case where $\rho_l = 0$, *Eq. 2.4* reduces to *Eq. 2.3b*. In this case, the critical volume fraction, where $\rho_m = 0$, is $\phi_c = L_\phi$, which is 1/3 for spheres.

The medium in the *Bruggeman's asymmetric theory* can be visualized as being made up of an infinite size range of uniformly coated ellipsoids, as illustrated for the case of spheres, in fig. 2.9. The volume ratio of the coating to the interior is the same for all ellipsoids. In the actual composite medium, the coating can be visualized as forming a host phase or matrix. On the other hand, the interior particles can be regarded as a dispersion. The complete Bruggeman's asymmetric equation, in the more general case where the conductivities of both phases have finite, nonzero values, is derived and given in Meredith et al. [84] and Landauer [88], as well as on a more rigorous basis in Sen et al. [87].

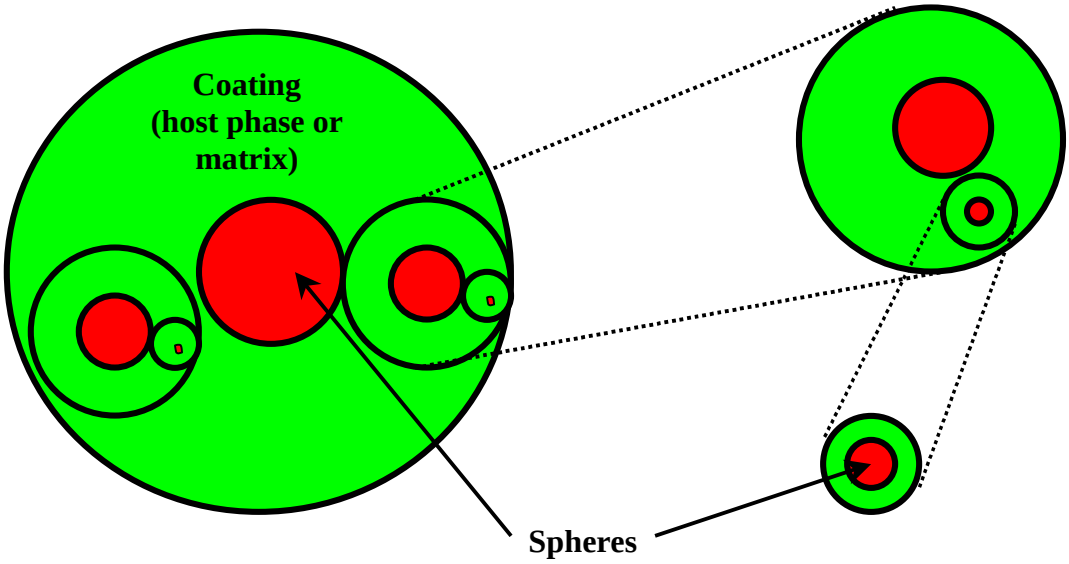

Figure 2.9. The Bruggeman's asymmetric medium made up of coated spheres (in red), with a very large range of sizes (from McLachlan et al. [80]).

When the conductivity of the dispersion is zero (σ_l = 0), the Bruggeman's asymmetric equation reduces to the following equations.

For oriented ellipsoids:

$$\sigma_m = \sigma_h(1 - f)^{1/(1 - L_f)} \text{.....} Eq.\ 2.5a.$$

For randomly oriented ellipsoids:

$$\sigma_m = \sigma_h(1 - f)^{m_f} \text{.....} Eq.\ 2.5b.$$

In equations 2.5a and b, f corresponds to the volume fraction of the insulating dispersion. When the conductivity of the dispersion is infinitely high the equation is better written in terms of the resistivities and the volume fraction (ϕ) of the perfectly conducting dispersion. Bruggeman's asymmetric equation then becomes:

For oriented ellipsoids:

$$\rho_m = \rho_h(1 - \phi)^{1/L_\phi} \text{.....} Eq.\ 2.6a.$$

For randomly oriented ellipsoids:

$$\rho_m = \rho_h(1 - \phi)^{m_\phi} \text{.....} Eq.\ 2.6b.$$

It should be noted that the above equations imply that there is no metal-insulator (Eqs. 2.5a and b) or conductor-perfect conductor (Eqs. 2.6a and b) transitions except where $f = 1$ (or $\phi = 1$), which implies that $f_c = 1$ (or $\phi_c = 1$) in these equations.

2.4.4 OTHER CONDUCTIVITY MODELS.

- The rule of mixtures. The simplest approach for the prediction of the electrical conductivity of a fully aligned continuous-fibre reinforced composite utilises either the rule of mixtures or the inverse rule of mixtures [83,92,93]. In both cases the composite is considered a network of electrical resistances. The equation giving the conductivity parallel to the fibre direction is based on a *parallel model.* In this case, the model describes a stack of slabs (or rods) of the two conducting media linked in parallel with the current flow. In terms of parameters already defined, the conductivity is given by:

$$\sigma_m = f\sigma_l + (1-f)\sigma_h \text{ .....} \textit{Eq. 2.7.}$$

On the other hand, the conductivity perpendicular to the fibre direction is given by an equation based on a *series model.* In this case, the model describes a stack of slabs (or rods) of the two conducting media linked in series with the current flow. For this case, the composite conductivity is given by:

$$\frac{1}{\sigma_m} = \frac{f}{\sigma_l} + \frac{1-f}{\sigma_h} \text{ .....} \textit{Eq. 2.8.}$$

- The grain consolidation model of Roberts and Schwartz [94]. This is a geometrical model proposed for diagenesis, which is the process by which granular systems evolve geologically from unconsolidated, high-porosity packings toward more consolidated, less porous, materials. It proposes that the relation between the conductivity and the porosity can be approximated by a non-trivial power law over a wide range of porosity for both ordered and disordered lattice configurations. In each case, the system initially consists of a tightly packed aggregate of hard spherical grains of uniform radius. As the system moves towards lower porosity, the grains are gradually distorted until, at the end of the process, they become a set of space-filling polyhedrons. The conductivity is modelled in relation to the nucleation of a random array of small insulating spheres

embedded in a biphasic-conducting composite. The starting biphasic phase, and the biphasic phase remaining after the pure insulating phase has started to grow, are treated as one phase. The second phase is the insulating spheres, which then grow to form a random-close-packed lattice with point contacts on the surfaces. As the radii of the insulating spheres increase further, the areas of interfacial contacts grow, creating an ever-decreasing volume of pores and "throats", which contains the remaining biphasic mixture. Finally, when the volume fraction of the insulating spheres (f) is about 0.97 [94], the throats no longer form a percolation path, which gives a percolation threshold (ϕ_c) of approximately 0.03.

- Segregated system models. The models are based on the prediction of the conductivity in composites consisting of mixtures of metal and insulating particles, in which the radius of the metal particles (R_M) is much smaller than that of the insulating particles (R_I). When such a type of mixture was subjected to compaction (Malliaris and Turner [95]), it was observed that the metal particles filled non-spherical voids between the insulating particles, which led to segregation of the metal. The analysis performed by Malliaris and Turner [95] on this type of system showed that ϕ_c reached a value of about 0.05 when the radius of the conducting particle was about 30 times smaller than that of the insulating particle. These researchers calculated the value of ϕ_c for R_I/R_M on the basis that each non-conducting grain was covered with a monolayer of conducting particles at ϕ_c. The metallic particles were thus envisaged as being located on planar lattices and it was assumed that the critical composition was possibly due to the initial formation of infinitely long sequences of contiguously occupied sites on the lattice. Kusy [96], however, realised that the conducting particles did not have to cover the insulating ones completely to form a percolation path. In this case, a two-dimensional percolating network was proposed to be formed at ϕ_c of about one half of that needed for the model of Malliaris and Turner. Kusy also realised that conducting particles, not on the surface of the insulating grains, but trapped in the interstitial sites or pores, increased the observed value of ϕ_c.

2.5 FIBRE FORMATION IN BINARY POLYMER COMPOSITES.

This section covers general concepts related with the formation of fibres in two-component polymer blends. Technical definitions, given in the context of the present work, are presented in section 2.5.1, whereas notions concerned with the morphology of binary polymeric systems are provided in section 2.5.2. A summary on some of the approaches used for the formation of fibres in polymer blends is also presented here.

2.5.1 IN-SITU COMPOSITES: DEFINITIONS.

A *composite* can be defined as the material created when two or more distinct components are combined. However, in the context of the present work, composites are those materials formed by aligning continuous fibres in a polymer resin matrix or binder. In general, the fibres are strong and stiff such that they are the principal load-carrying members whereas the surrounding matrix, that keeps them in the desired location and orientation, acts as a load transfer medium between them. At the same time, the matrix protects the fibres from environmental damage. In this case, the material has exceptional mechanical properties and is often termed as an advanced, or *fibre reinforced composite* [97-100]. At present, this class of materials is important in engineering applications previously dominated by metals. For example, laminates are widely used with structural functions. However, difficulties are present in terms of the prolonged fabrication times associated with combining the fibre reinforcement and matrix so as to give predictable properties in the final product. Moreover, even in the case when short-fibre reinforced thermoplastics are processed by extrusion and injection moulding difficulties still remain in controlling the fibre length distribution and orientation in finished parts. Additionally, the increased viscosity of the melt due to the incorporation of the fibres is another problem that has to be taken into consideration [101].

An approach to avoid some of the aforementioned difficulties is the production of *in-situ composites*, in other words, to generate the fibres during the actual forming process of the component. To achieve this, the study of the rheological properties and microstructure of extruded specimens of binary blends should be considered. This has been extensively investigated and it has been shown that under appropriate conditions,

the dispersed phase can deform during processing to produce elongated structures, e.g., ellipsoids or even fibres [102-108]. A general review on the rheology of polymer blends is available in section 2.6.

Another area of research relevant to the study of in-situ composites is the processing method used for their production. A variety of techniques have been developed in the past, including capillary extrusion [109], uniaxial drawing [110], gel spinning methods [111], etc..

2.5.2 MORPHOLOGY OF BINARY POLYMER BLENDS.

The morphology of a binary blend is initially dependent on the way in which the two components flow during forming. Two types of multiphase flow may be distinguished on the basis of their degree of phase separation. One type is dispersed multiphase flow, in which one component exists as a discrete phase dispersed in another component forming the continuous phase. The other type is stratified multiphase flow, in which two or more components form continuous phases separated from each other by continuous boundaries [101].

In general, only dispersed multiphase flow is of relevance when applied to the in-situ formation of fibres of one polymer in a blend. Depending on the nature of the discrete phase, the bulk flow properties of a dispersed multiphase system may vary. In other words, the bulk flow properties of a dispersion can be different depending on whether the dispersed phase consists of rigid particles, deformable droplets, or even gas bubbles suspended in the continuous polymeric medium. In the processing of heterogeneous polymer blends, both phases are usually non-Newtonian and viscoelastic. When two polymers of different structure are melt-blended it is common for one polymer to form a discrete phase within the other, giving rise to a two-phase system. In dispersed multiphase systems, there are many variables interrelated to each other, which affect the ultimate physical/mechanical properties of the final product. For instance, the method of preparation (the method of mixing the polymer blend) controls the morphology (e.g., the state of dispersion, particle size and particle shape) of the mixture. On the other hand, the rheological properties strongly dictate the choice of processing conditions (e.g., temperature, shear stress), which in turn strongly influence the

morphology, and therefore the ultimate physical/mechanical properties of the final product.

2.5.3 IN-SITU CRYSTALLISATION.

The earliest approach to the formation of in-situ composites was the concept of in-situ crystallisation. In this approach, an additive is introduced into the polymer, which is molten at the processing temperature. The reinforcing elements grow into elongated crystals within the amorphous matrix during the crystallization process. For example, Siegmann et al. [112] have added 2,4,5,6-tetrachloroxylene or 1,2,4,5-tetrachlorobenzene to ordinary and high-impact polystyrene. They observed that the additive precipitated in three different morphologies depending on the crystallization temperature: regular needles with aspect ratio of approximately 10, dendritic structures, and tiny crystallites as the crystallization temperature decreased. Although their primary interest was the production of a fine and uniform dispersion of the additive in a desired morphology, they noted that crystallization under shear could produce oriented needles of the additive.

Another account is given by Joseph et al. [113], who added acetanilide or anthracene to styrene-acrylonitrile copolymers. They also observed large, regular needles and dendritic structures at high and medium crystallization temperatures; but at the lowest temperature they found very long, thin needles.

2.5.4 IN-SITU POLYMERISATION.

The extension of in-situ crystallisation is the concept of in-situ polymerisation, in which needle-like crystals of a monomeric species are formed during processing, followed by further polymerisation of the monomer to obtain a highly oriented fibrous polymer. For example, trioxane has been crystallised and further solid-state polymerised (by gamma radiation) in a matrix of polycaprolactone or poly(ethylene oxide) [114]. On the other hand, monomers with conjugated triple bonds (e.g., di-and tri-acetylenes) have been used to form fibrillar extended-chain polymeric single crystals with very high modulus and tensile strengths [115].

2.5.5 BLENDS CONTAINING THERMOTROPIC LIQUID CRYSTALLINE POLYMERS.

It has been demonstrated [104,116-119] that the so-called thermotropic liquid crystalline polymers (LCPs) play an important role in generating the reinforcing species. Thermotropic LCPs are special type of thermoplastics having long-chain molecules, usually fully aromatic polyesters, which have sufficient chain stiffness to give extremely high strength, and yet have sufficient flexibility to melt. Thermotropic polymers form fibres extremely readily, even in injection-moulded parts. Molecular orientation occurs and the physical properties of moulded articles exhibit a high degree of anisotropy. For instance, studies performed by Chung [104] on LCP-Nylon 12 blends using various techniques, demonstrated that the LCP behaved like reinforcing fibre elements in the matrix.

Another account is given by O'Donnell et al. [117]. Their work consisted in exploring the effect of a compatibilizer (i.e., maleic anhydride-grafted polypropylene, MAP) on the properties of polypropylene (PP)-LCP blends. This study showed that MAP lowered the interfacial tension for all the PP-LCP blends, indicating that MAP compatibilized the PP-LCP blends. However, while in most polymer blends compatibilization leads to finely dispersed drops of the minor components, LCP fibrils were obtained over a large range of compatibilizer concentrations. Isolation of the PP-MAP phase from the LCP phase indicated that MAP did not react with the LCPs. Instead, an interaction such as hydrogen bonding was believed to be responsible for the compatibilization effect of MAP on the PP-LCP blends. The LCPs used in this work were poly(ester amide) and two copolyesters (Vectra® A950 and Vectra® B950).

Further investigations have been effectuated by Wong et al. [116] on the microstructure generated by reinforcing pre-compounded polycarbonate (PC)-polybutylene terephthalate (PBT) blends with a LCP (Vectra® B950). Injection moulded PC-PBT-LCP in-situ ternary composites were processed under a simple compounding procedure and the microstructural analysis showed that good fibrillation of LCP domains could be observed in 4-mm-thick dumbbell-shaped bars. Fibrillation also appeared to increase with the LCP content.

2.5.6 FIBRILLATION IN THE FLOW OF MOLTEN POLYMER BLENDS.

Evidence of fibrillation in the flow of polymer blends is widespread in studies that are concerned with the microstructure and rheological properties of melt processed blends of polymers. For example, studies performed by Folkes et al. [103] about the resulting microstructure of extruded samples of SBS block copolymer-polystyrene blends, revealed that the homopolymer polystyrene formed a separated phase, which in some cases was in the form of well-developed fibrils aligned parallel to the extrusion direction. Similar micro-morphology was observed by Ehtaiatkar et al. [102] in extruded specimens of SBS block copolymer-polyethylene blends. In this work, the careful control of the blending process and subsequent extrusion led the dispersed polyethylene to form well-developed fibres aligned parallel to the extrusion direction. Ehtaiatkar and co-workers concluded that these fibres were produced primarily as a result of the elongational flow field pertaining at the die entrance and by lowering of the surface energy of the polyethylene by the block copolymer matrix.

In a similar way, Boyaud et al. [120] report on the elaboration of an in-situ composite consisting of ethylene vinyl acetate copolymer (EVA) and polybutylenetherephtalate (PBT). In this work, an inter-chain chemical reaction during the processing operations was used to generate a grafted PBT-g-EVA copolymer at the interface of the two polymers. A morphology consisting of PBT fibres in the EVA matrix was achieved by stretching the extruded blend at the exit of the die.

On the other hand, Virtanen et al. [28] and Passiniemi et al. [121] give an account of the production of conducting PANI-polypropylene fibres in industrial scale processing equipment. The fibres were spun at speeds of up to 1000 m/min with subsequent orientation. The composite, characterised by transmission electron microscopy, showed a unique morphology with a phase separated continuous conductive PANI-network embedded in the polypropylene matrix.

2.6 FACTORS AFFECTING THE MORPHOLOGY OF POLYMER BLENDS DURING MELT PROCESSING.

Polymer blends may be classified as miscible or immiscible. The behaviour of the former is similar to that of a homopolymer or a random copolymer. The immiscible

systems are frequently characterized by more than one glass transition temperature. Their properties, to a great extent, are controlled by their morphology, which in turn depends on the thermodynamic and rheological properties, as well as on deformation and thermal history. The multiphase nature of polymer blends and variation of their structure imply that flow responses may be complex. Therefore, during processing and fabrication of blends, not only the parameters controlling homogeneous polymer systems (e.g., molecular weights, their distribution, as well as thermal and stress histories) must be considered, but also the morphology and its evolution.

Theoretical and experimental studies indicate that the morphology of a polymer blend is determined by parameters such as interfacial tension, viscosities of the materials, composition and processing conditions including temperature, residence time, flow patterns and shear rate levels [120,122-126].

The theories developed to describe the deformability of the dispersed phase in a binary blend are mostly concerned with Newtonian systems. However, these can be used as general guides to describe the deformability in pseudoplastic systems. This section thus provides a brief discussion of the classical theory of droplet deformation and break up in Newtonian systems. A short review on the basic physical properties that control the size and shape of the dispersed phase under melt processing conditions is also presented. Finally, factors affecting the control of the shape are also considered here in a section devoted to droplet-fibre transitions.

2.6.1 THEORY OF DROPLET DEFORMATION AND BREAKUP.

When a neutrally buoyant, initially spherical droplet is suspended in another liquid, and subjected to shear or elongational stress, it deforms and then breaks up into smaller droplets. Taylor extended the work of Einstein on dilute suspensions of solid spheres in a Newtonian liquid, to dispersion of a single Newtonian liquid droplet in another Newtonian liquid subjected to a well-defined deformational field (refer to Utracki et al. [123] and the references cited therein). It was noted that at low deformation rates in both shear and elongational (or hyperbolic) flow fields, the sphere deformed into a spheroid (fig. 2.10).

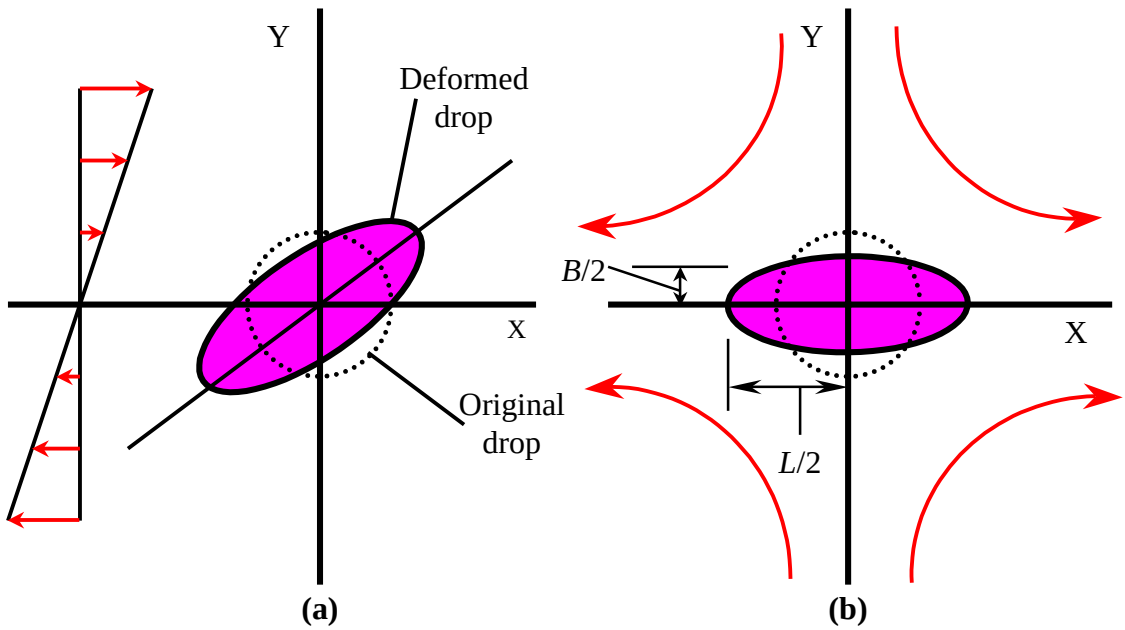

Figure 2.10. Schematics of droplet deformation in uniform shear (a) and in plane elongational (b) flow fields (from Utracki et al. [123]). The red arrows indicate the flow direction. *L* and *B* are the major and minor axes of the ellipsoid, respectively.

The velocity and pressure fields inside and outside the droplet were calculated, suggesting that at low stresses in steady uniform shearing flow the deformation degree, *E*, could be expressed by means of two dimensionless parameters (*Eq. 2.9*), namely the capillary (or Taylor) number, *Ca*, and the ratio of the viscosity of the dispersed phase to that of the matrix, *p*.

$$E = Ca[(19p + 16)/(16p + 16)] \text{.....} Eq.\ 2.9.$$

In equation 2.9,

$$Ca = \frac{\eta_m R \dot{\gamma}}{\alpha} \text{.....} Eq.\ 2.9a,$$

and

$$p = \eta_d / \eta_m \text{.....} Eq.\ 2.9b,$$

where η_m is the viscosity of the matrix, $\dot{\gamma}$ is the shear rate, *R* is the droplet radius, α is the interfacial tension coefficient and η_d is the viscosity of the dispersed phase. Taylor showed that at breakup, the apparent deformation, *D*, of the droplet (*Eq. 2.10*) has a value of 0.5.

$$D = (L - B)/(L + B) \text{.....} Eq.\ 2.10.$$

In equation 2.10, L is the major axis of the ellipsoid represented in fig. 2.10, whereas B is its minor axis. Theoretically, at droplet breakup, E also has a value of 0.5. Taylor then demonstrated experimentally that for values of p from 0.1 to 1, droplet breakup occurred at D values between 0.5 and 0.6. Equation 2.9 indicates that the viscosity ratio (p), the shear rate, the droplet diameter and the interfacial tension are critical variables to consider in controlling particle deformation and breakup in Newtonian fluids.

Experimental studies performed by Grace [127] showed that p and Ca are related and that the possibility for the drop to sustain deformation without break up is given by an empirical critical capillary number, Ca_{crit}, that has to be compared with the actual local capillary number. It was observed that by increasing the capillary number, the drop deformation increased linearly with Ca. Above Ca_{crit}, the particles broke up into small droplets. Grace [127] and many subsequent authors have shown that Ca_{crit} depends not only on p but also on the nature of the flow. In the shear field, when $p > 4$, viscous drops never break. Instead, they deform into fibres and then rotate in the flow field. In contrast, viscous drops subjected to an elongational flow field can break for any value of p, providing that $Ca > Ca_{crit}$. Furthermore, it was also found that it is easier to break drops when $p = 1$. In consequence, it was found that an elongational flow field was much more effective for droplet breakup than a uniform shear flow field (fig. 2.11).

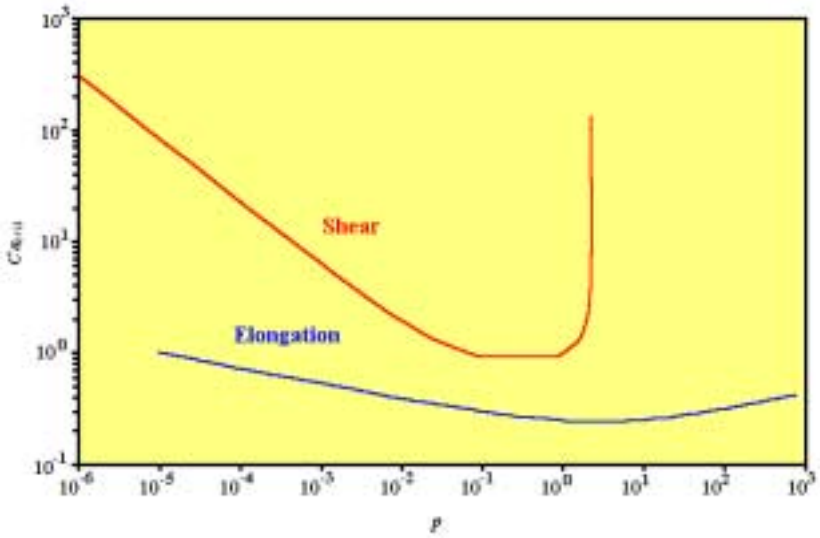

Figure 2.11. Typical variation of the critical capillary number, Ca_{crit}, with respect to the viscosity ratio, p, in simple shear and elongational flow (from Favis [125]).

Figure 2.11 shows that droplets are stable when their *Ca* number is below the critical value; deformation and breakup of a droplet is easiest at values of *p* around 0.25 – 1 for shear flow; and elongational flow is more effective for breakup and dispersion than is shear flow.

The drop deformation and breakup are transient phenomena in a sense, and they require a specific time that must be defined. With respect to this, observations on the disintegration of a deformed fine thread into a series of fine droplets led to a definition of the time required for thread breakup. The phenomenon previously described is known as capillary instability and is often observed under transient shear conditions or after cessation of flow (refer to Utracki et al. [123], Favis [125], and the references cited therein). Accordingly, in a dimensionless form, the time scale can be defined as follows:

$$t_{crit} = \frac{t_b \dot{\gamma}}{Ca} \quad \text{.....Eq. 2.11,}$$

where t_b is the breakup time under quiescent conditions via Rayleigh disturbances, which can be expressed as:

$$t_b = \frac{\eta_m d_o}{\alpha \Omega(\lambda, p)} \ln\left(\sqrt{\frac{1}{6}} \frac{d_o}{\xi_o}\right) \quad \text{.....Eq. 2.12,}$$

where d_o is the initial thread diameter, ξ_o is the initial amplitude of the sinusoidal disturbances, and Ω is a tabulated function of *p* and the characteristic wavelength, λ, of the disturbances (refer to fig. 2.12).

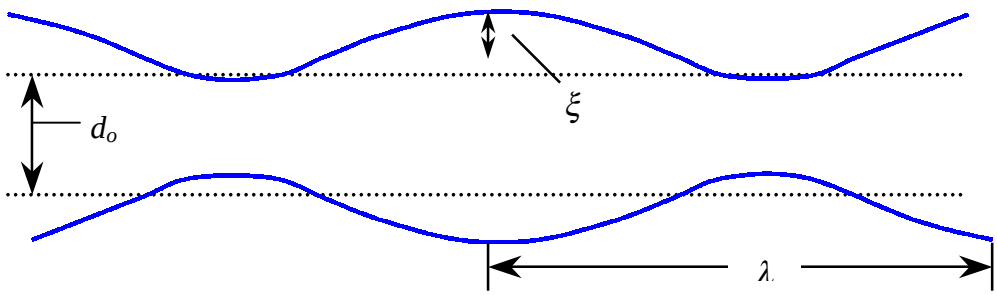

Figure 2.12. Sinusoidal Rayleigh disturbance of a thread with d_o = initial thread diameter, ξ = amplitude of the sinusoidal disturbances and λ = the distortion wavelength (from from Utracki et al. [123]).

2.6.2 VISCOSITY RATIO.

The viscosity ratio (*p*) has been shown to be one of the most critical variables for controlling blend morphology. Generally, if the minor component has a lower viscosity than the major one, the minor component will be finely and uniformly dispersed. Conversely, the minor component will be coarsely dispersed if its viscosity is higher than that of the major component. For example, Favis et al. [128] have shown that for polycarbonate (PC)-polypropylene (PP) blends, the viscosity ratio had a marked effect on the morphology of the dispersed phase (PC), with the size of the latter increasing with the increase of *p*. Favis and co-workers carried out their studies using an internal mixer chamber. They observed that when the torque ratio (i.e., the ratio of the torque generated by the dispersed phase to that generated by the matrix) increased from 2 to 13, the size of the PC phase increased by a factor of 3 to 4. Reduction of the size of the minor phase was achieved below a torque ratio of 1, with a minimum particle size occurring at a torque ratio of approximately 0.25. Subsequent work has shown that the breakup of the dispersed phase in PC-PP blends of a higher *p* is much more efficient in twin-screw extrusion than in an internal mixer [129].

In the case for which capillary instabilities play an important role, the mechanism controlling the influence of the viscosity of the components can be quite different. Equation 2.12 demonstrates that a matrix with a higher viscosity will stabilize the fibre against capillary instabilities. Increasing the viscosity ratio of the system leads to a significant increase in thread breakup time [130,131]. In studying the initial mixing of two immiscible fluids in a two-dimensional rectangular cavity, Kang et al. [132] reported that the transient breakup process was more dependent on the matrix viscosity than on the viscosity ratio. A higher matrix viscosity resulted in a more evenly distributed dispersion because it delayed the breakup time.

2.6.3 COMPOSITION.

The final morphology is a balance between deformation and disintegration phenomena on one hand, and *coalescence* on the other. For this reason, various morphological structures are obtained by varying the composition [125]. Increasing the fraction of the dispersed phase results in an increase in the particle size due to

coalescence. To visualize the coalescence phenomenon, one must consider the collision of two identical particles in shear flow. Thus, coalescence can be considered to take place in the following manner: First, upon collision, the particles deform, and matrix material is expelled from the region between them. The drops then burst, a neck is formed, and finally, the two drops coalesce into one particle. Various parameters determine the extent of coalescence. The basic ones are the volume fraction of the dispersed phase, the radius of the particle, the viscosity of each phase, and the interfacial tension, which is the ultimate driving force for coalescence.

2.6.4 SHEAR STRESS.

In general, it has been demonstrated that an increase in the shear stress would result in a decrease of the droplet size. For instance, Min et al. [133] noted that in a system polyethylene (PE)-polystyrene (PS), shearing at high levels of stresses resulted in much finer phase morphology. In this case, the shear stress appeared to predominate over the viscosity ratio, since variations in the molecular weight of the PE or in the mixing temperature, which are expected to influence the viscosity ratio, did not influence the scale of the morphology. There is general agreement, however, that large variations in the shear stress are required for it to predominate over the viscosity ratio in controlling the dispersed-particle size (refer to Favis [125] and the references cited therein).

On the other hand, modifying the applied shear stress can influence the shape of the dispersed phase. For example Gonzalez-Nunez et al. [134], report that an increase in the shear stress from 17kPa to 29kPa resulted in a change in the shape of the dispersed phase in nylon-6-PE blends prepared by extrusion through a slit die. At lower shear stresses, the nylon phase was dispersed in the PE matrix in the form of spherical particles. However, increasing the shear stress resulted in higher deformation of the dispersed phase and a fibre-like dispersed phase was formed.

2.6.5 INTERFACIAL MODIFICATION.

Interfacial modification appears to be a dominant factor for controlling the dispersed-phase size. Even the phase-size versus viscosity ratio dependence is less pronounced for compatibilized systems [135].

In most cases, compatibility is enhanced by the use of block or graft copolymers with particular segments that are capable of physical and/or chemical interactions with the blend components. Block copolymers are typically designed so that a given block is miscible with a given phase. If the block copolymer locates at the interface, it will weave in and out of each phase, essentially binding the two components together.

The principal effects of interfacial modification on the morphology in an immiscible blend are to reduce the particle size and to narrow the particle-size distribution [136,137]. This reduction in particle size is related to both a decrease in interfacial tension and reduced coalescence.

Cigana et al. [138] showed that coalescence was suppressed in a blend of ethylene-propylene rubber (EPR) with PS on addition of a tapered styrene-ethylene butylene (SEB) diblock copolymer interfacial modifier, whereas the uncompatibilized system demonstrated measurable coalescence at concentrations above about 5 % of the dispersed phase.

Fayt et al. [139], have extensively studied block copolymers as interfacial modifiers under melt-mixing conditions. They have shown that the mechanical performance of PE-PS blends is highly dependent on the molecular characteristics of the copolymers. Over a broad range of molar mass, they reported that diblocks are more effective than graft, triblock, or star-shaped copolymers. Diblock copolymers with a balanced composition appeared to be the most efficient interfacial agents.

2.6.6 DROPLET-FIBRE TRANSITION.

In order to develop fibre-like morphologies, the particles must be deformed and the shape must be maintained. Deformation phenomena, capillary instabilities, coalescence and the state of the interface are important parameters to consider if fibre-like morphologies are desired.

As already mentioned, the type of flow field present in melt processing greatly influences the mechanism of minor-phase deformation. Elongational flow fields have proven to be more effective in deforming particles than shear flow fields, although significant stretching into cylindrical bodies can also be obtained under conditions of rapidily changing shear rates. The fibrillar morphology that is often observed in immiscible blends near the die wall is an example of the latter case.

Evidence of fibrillation in the flow of molten mixtures of polymers was first presented by Tsebrenko et al. [140] who examined the morphological state of polyoxymethylene (POM)/copolyamide (CPA) blends. The two thermodynamically incompatible polymers were blended and then extruded through a capillary die and examined at various points along the die by freezing samples in liquid nitrogen. Micrographs collected just past the die entrance indicated very little orientation of the dispersed POM phase within the CPA phase. However, the extrudate collected at the downstream side of the die showed that fine, well-oriented fibrils of POM existed in the in the CPA matrix. As an explanation for the occurrence of the fibrillation observed, Tsebrenko and co-workers presented the schematic shown in figure 2.13.

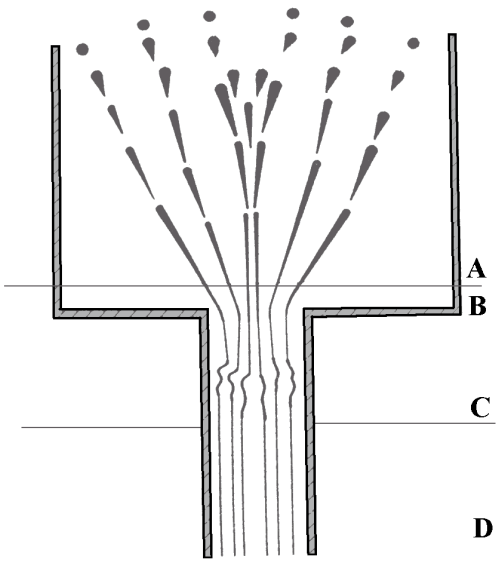

Figure 2.13. Representation of the fibrillation process in the entrance zone and in the ducts (from Tsebrenko et al. [140]).

In figure 2.13, the dispersed droplets, formed initially during the mixing operation, are elongated as they enter the die entrance (region A) under the effect of tensile stress acting in the direction of the converging streamlines. The elongated

droplets then recoil as they pass the die entrance (region C). Finally, rearrangement of the elongated droplets occurs at the downstream side of the capillary (region D), giving rise to the fibrils parallel to the capillary axis. The final extrudate was therefore reinforced with uniaxially aligned fibres. The results indicate that the formation of thin fibrils takes place at the die entrance and that a prerequisite for the production of continuous fibrils is the existence of a tensile stress acting on the fibrils in the entrance zone.

The efficacy of elongational flow in provoking droplet-fibre transitions has been confirmed in numerous studies. Dreval et al [141] observed that fibre formation was enhanced during extrusion at the entrance of the capillary, where contraction generates an elongational flow. They found that the fibre formation occurred at specific values of the viscosity ratio and the extrusion speed. The elongational flow generated during uniaxial melt drawing is also very effective in forming dispersed fibres [134,142]. Delaby et al. [143] studied the deformation of dispersed droplets in immiscible blends in elongational flow. They developed a method for quenching the sample after subjecting it to a controlled flow in the melt and investigated the influence of the viscosity ratio for a range of capillary numbers. Their results indicate that the drop deforms less than the sample when it has a viscosity higher than that of the matrix. On the other hand, the drop deformed more than the sample when its viscosity was lower than that of the matrix.

In capillary flow, the length of the capillary plays an important role in the conservation of an extended morphology. LaMantia et al. [144] showed that LCP fibres, initially formed in the converging region of the capillary, retained their shape when extruded in a capillary with a length (L) to diameter (D) ratio almost equal to zero. However, when a capillary with L/D = 40 was used no elongated LCP particles were observed. The loss of the fibrillar form during flow through a long capillary was attributed to high shear, which causes breakup of the fibrils, and to an orientation relaxation time of the LCP less than the average time for the polymer to flow through the capillary. Chapleau et al. [145] reported similar behaviour for blends of 5 % of PC in PP. It was found that extrusion through dies with a high L/D resulted in dispersed PC droplets, whereas the use of a capillary with L/D = 0.73 resulted in a fibrillar dispersed phase.